BUTTERWORTH HEINEMANN

Polymer Vol. 36 No. 17, pp. 3267–3271, 1995

0032-3861/95/$10.00+0.00

Pressure dependence of the elastic constants of poly(methyl methacrylate)

K. Weishaupt*, H. Krbecek and M. Pietralla
Abt. Experimentelle Physik, Universität Ulm, D-89069 Ulm, Germany

and H. D. Hochheimer
Department of Physics, Colorado State University, Fort Collins, CO 80523, USA

and P. Mayr
Abt. Angewandte Physik, Universität Ulm, D-89069 Ulm, Germany
(Received 24 October 1994)

We report measurements of the hydrostatic pressure dependence of the elastic constants of poly(methyl methacrylate) using high resolution Brillouin spectroscopy. We have measured the density $\rho(p)$ up to 500 MPa, and the longitudinal and transverse sound velocities up to 300 MPa. We have calculated the bulk modulus, Youngs modulus, shear modulus and Poisson's ratio. Initially there is a strong increase in the intensity of the shear phonons which levels off at $p > 100$ MPa. At this pressure a dispersion-like step in the shear modulus as well as a decrease in the bulk modulus is found, which is tentatively discussed as a 'weak glass transition' within the glass.

(Keywords: poly(methyl methacrylate); elastic constants; high pressure)

INTRODUCTION

There is great interest in the understanding of the glass transition process. Thus, much effort has been directed towards theoretical approaches and computational simulations. Many published works report the temperature dependence of the specific volume, the relaxational behaviour and even high frequency elastic constants, thereby allowing theories and simulations to be tested. But the glassy state itself also deserves closer inspection.

One way to characterize a glass is via the amount of free volume. Therefore pressure experiments in which the specific volume is changed isothermally should provide more insight into the properties of the glassy state. Pressure changes are more powerful than temperature changes[1]. However, reports on the pressure dependence of the properties of these materials are scarce. Most experiments published were performed near and above the primary glass transition in order to investigate its pressure dependence. There are some studies which use the pulse-echo overlap technique (e.g. ref. 2) to measure the sound velocity in the glass and hence the initial pressure derivative of the bulk modulus. Using the 'natural velocity' technique, these authors could not give the pressure dependence of the elastic constants. As we have measured the pressure dependence of the density $[\rho(p)]$ by dilatometric techniques and the pressure dependence of the longitudinal and transverse velocities $[v_L(p), v_T(p)]$ by Brillouin scattering experiments, we are able to determine the pressure dependence of the bulk modulus B_s, shear modulus G, Young's modulus E and Poission's ratio ν, which are given by:

$$B_s = c_{11} - \tfrac{4}{3}c_{44} \tag{1}$$

$$E = \frac{c_{44}(3c_{11} - 4c_{44})}{c_{11} - c_{44}} \tag{2}$$

$$G = c_{44} \tag{3}$$

$$\nu = \frac{c_{11} - 2c_{44}}{2(c_{11} - c_{44})} \tag{4}$$

EXPERIMENTAL

First, we measured the pressure dependence of the density ρ of poly(methyl methacrylate) (PMMA) (Plexiglas®, Röhm GmbH) using a high pressure dilatometer as described in ref. 3. The specimens had a cylindrical shape, 100 mm long and 22 mm in diameter. With these data and the index of refraction $n_{514\,nm} = 1.491$ at normal conditions (21°C), measured with an Abbe refractometer, we can calculate the pressure dependence of the refractive index by using the constancy of the specific refraction, r, given by[4]

$$r = \frac{(n^2 - 1)}{\rho(n^2 + 2)} \tag{5}$$

Cubic specimens measuring approximately 5 × 5 × 5 mm were cut from the same material, and used for the Brillouin experiments. The faces were polished to a very high optical quality and therefore produced low Rayleigh scattering intensity.

* To whom correspondence should be addressed

All experiments were performed at room temperature (294 ± 0.5 K). As light source we used the 514 nm line of a single-mode argon-ion laser. To avoid heating and damage of the sample, the power of the laser beam passing through it did not exceed 100 mW.

The Brillouin measurements were performed with the four-pass Fabry–Perot interferometer of a 4/2-pass Sandercock tandem interferometer. The free spectral range was set to 15 and 15.5 GHz up to 275 MPa, and to 11.34 GHz above 275 MPa. A three-window optical high-pressure cell as described in ref. 5 was used with synthetic oil (Plexol) as pressure medium, using the index matching technique. After each pressure step we waited 1 h prior to data acquisition, in order avoid non-equilibrium effects. After subtracting a constant background from the measured spectra, the Rayleigh lines were fitted by a sum of Lorentz and Gauss functions. With fixed parameters for the Rayleigh lines, all Brillouin lines were then fitted to give the frequency shifts and the integral intensities. We calculated the sound velocities v_i ($i = \mathrm{T}, \mathrm{L}$) using the relation for the Brillouin shifts, Δv_i

$$\Delta v_i = \pm 2 \frac{n v_i}{\lambda_0} \sin\left(\frac{\theta}{2}\right) \tag{6}$$

where n is the index of refraction, λ_0 is the wavelength of the incident light and θ is the inner scattering angle. Using an 90°N scattering geometry[6], equation (6) becomes

$$\Delta v_i = \pm \sqrt{2} \frac{n}{\lambda_0} v_i \tag{7}$$

From the pressure dependence of the transverse and longitudinal sound velocities, the pressure dependence of the elastic constants of isotropic media can be calculated using

$$\begin{aligned} c_{11} &= v_{\mathrm{L}}^2 \rho \\ c_{44} &= v_{\mathrm{T}}^2 \rho \end{aligned} \tag{8}$$

provided the pressure dependences of the density ρ and the index of refraction are known.

RESULTS

The data at ambient pressure are listed in *Table 1* (see also ref. 7).

Density

Figure 1 shows the density *versus* pressure data. The data can be fitted to a polynomial of sixth degree

$$\rho(p) = \sum_{k=0}^{6} a_k p^k \tag{9}$$

The deviations from this fit are also plotted in *Figure 1* and are <0.15% in the whole pressure range. The constants a_k are given in *Table 2*.

Using the specific refraction at ambient pressure, we have calculated the refractive index as a function of density. According to theory, the specific refraction is a molecular constant of the monomer provided the average spatial correlations of the molecular constituents do not change. Indeed, only very small changes of the molecular polarizability with increasing pressure have been observed. They affect the refractive index in the order of one part in 10^4 (ref. 8). This influence appears to be negligible compared with the effects observed.

Table 1 Numerical values of different properties at zero applied pressure

v_{L} (m s^{-1})	2780
v_{T} (m s^{-1})	1410
c_{11} (GPa)	9.13
c_{44} (GPa)	2.40
B_{s} (GPa)	5.93
E (GPa)	6.34
ν	0.327

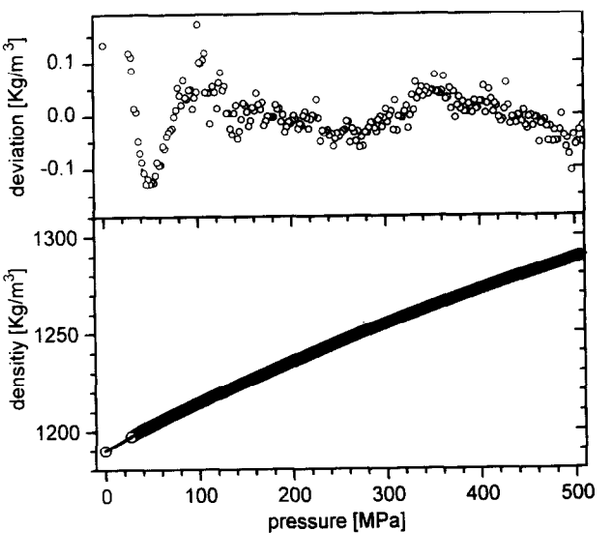

Figure 1 Lower part: density of PMMA *versus* pressure at $T = 21 \pm 0.5$°C (○, measurements; ——, fit). Upper part: deviations from the fit function (equation (9)), the parameters of which are listed in *Table 2*. The relative deviations are smaller than 1.5×10^{-4}

Table 2 Numerical values of the polynomial representation of $\rho(p)$, equation (9)

a_0 (kg m^{-3})	1190
a_1 (s^2 m^{-2})	0.2896
a_2 (s^4 m^{-1} kg^{-1})	-6.653×10^{-4}
a_3 (s^6 kg^{-2})	2.875×10^{-6}
a_4 (m s^8 kg^{-3})	-7.305×10^{-9}
a_5 (m^2 s^{10} kg^{-4})	9.254×10^{-12}
a_6 (m^3 s^{12} kg^{-15})	-4.632×10^{-15}

Sound velocity

Spectra from Brillouin scattering experiments are shown in *Figure 2* at 0.1 (ambient pressure), 60 and 210 MPa. Several features can be seen: (1) a shift of the peak position of the longitudinal as well as the transverse phonons and (2) an enormous increase of the intensity of transverse phonons compared with the longitudinal ones.

The spectra were analysed by simultaneously fitting all observed features. The line shifts determined were used to determine the elastic constants using equations (7) and (8). The pressure dependences of these constants are displayed in *Figure 3*. The data for c_{11} can be fitted to

$$c_{11}(p) = c_{11}^0 + \left.\frac{\mathrm{d}c_{11}}{\mathrm{d}p}\right|_{p=0} p + bp^2 \tag{10}$$

(with $c_{11}^0 = 9.13\,\text{GPa}$, $dc_{11}/dp|_{p=0} = 18.8$ and $b = -7\,\text{GPa}^{-1}$) and for c_{44} to

$$c_{44}(p) = c_{44}^0 + \left[(s_1 - s_2)\left(1 + \exp\frac{p - p_0}{\Delta p}\right)^{-1} + s_2\right]p \tag{11}$$

(with $c_{44}^0 = 2.40\,\text{GPa}$; s_1, s_2, p_0 and Δp are given in *Table 4*).

The elastic constant c_{11} increases uniformly, whereas c_{44} exhibits two different slopes at low and high pressures with a crossover at about 110 MPa. This is an important result, because this change is transferred to all other derived properties. The accuracy of the Brillouin and density data (uncertainty <1%) mean that the effect is genuine. A wrong assignment of phonons can also be excluded.

The step-like behaviour of c_{44} is also reflected by the strong increase of the intensity of the observed transverse phonon lines. For a cubic or isotropic body the intensity ratio of longitudinal and transverse phonons is given by

$$\frac{I_T}{I_L} = \left(\frac{V_L}{V_T}\right)^2 \left|\frac{p_{44}}{p_{12}}\right|^2 \tag{12}$$

where p_{ij} are Pockels coefficient. Since the absolute intensity of the longitudinal phonons remains about constant, the increase is due to an enhancement of the cross-section of transverse phonons described by the Pockels coefficient p_{44}. It describes the change in polarizability induced by a shear wave. The ratio $(p_{44}/p_{12})^2$ is plotted in *Figure 4*. It exhibits a strong increase at lower pressures and approaches a constant value above 125 MPa after going through a small maximum at about 110 MPa. The reason for the maximum could be a greater uncertainty because of a partially overlap of the Stokes and Antistokes transverse lines in this pressure region.

To a first approximation an ideal shear of particles does not change the polarizability[9]. Hence, shear phonons can hardly be observed in glasses. However, if the shear couples to rotations through anisometric molecular moieties, the polarization change by rotation enhances p_{44} significantly. An example is given in the case of polycarbonate, where transverse phonons have been investigated[10] and observed even in the molten state[11].

The moduli calculated using equations (1)–(3) are plotted in *Figure 5*, and the Poisson's ratio v is given in *Figure 6*. With increasing pressure v decreases linearly from quite a common value for polymers at normal pressure[7]. At about 110 MPa it drops significantly and then decreases further with a larger slope to values as low as 0.14 (the value for vitreous silica at room temperature) at $p = 200\,\text{MPa}$. This indicates that a large transverse

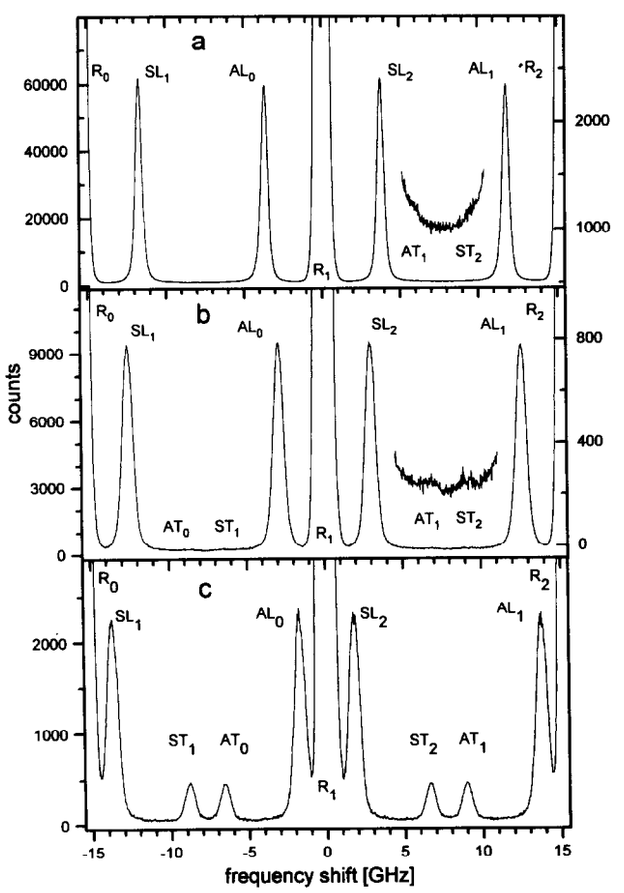

Figure 2 Unpolarized spectra of PMMA: (a) at ambient pressure, accumulation time = 4 h (*y*-axis at the right-hand side refers to the inset; (b) at 60 MPa, accumulation time = 1 h 20 min; (c) at 210 MPa, accumulation time = 25 min. L = longitudinal, T = transverse, R = Rayleigh, S = Stokes, A = Antistokes, the numbers indicate the order of the line

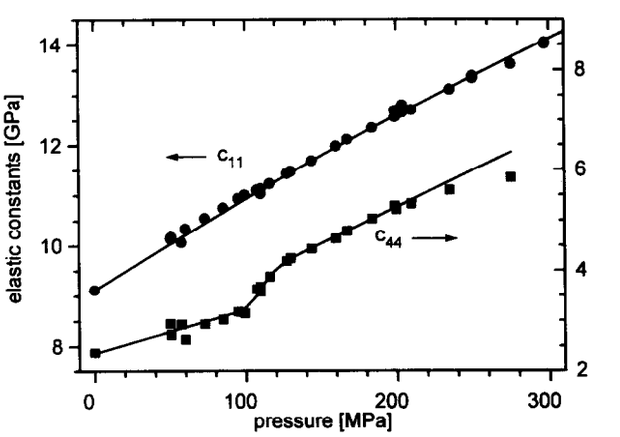

Figure 3 Elastic constants c_{11} and c_{44} of PMMA *versus* pressure. The solid lines represent fits to equations (10) and (11)

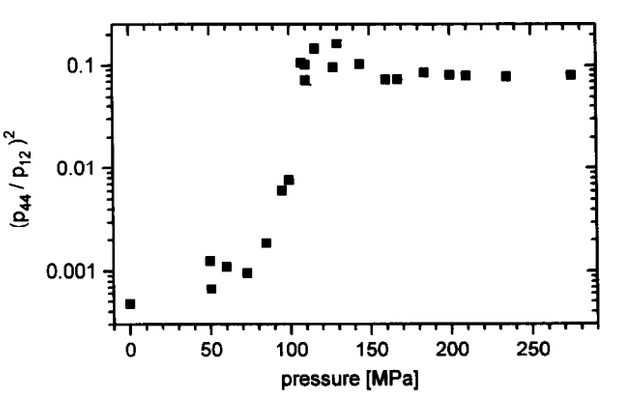

Figure 4 Ratio of Pockels coefficients $(p_{44}/p_{12})^2$ *versus* pressure, reflecting the change in scattering cross-section and showing the development of the new state at 110 MPa. There is a small increase from 6.7×10^{-4} at ambient pressure to 7.6×10^{-3} at 99.5 MPa, which is followed by a significant step to an almost constant value at pressures >125 MPa

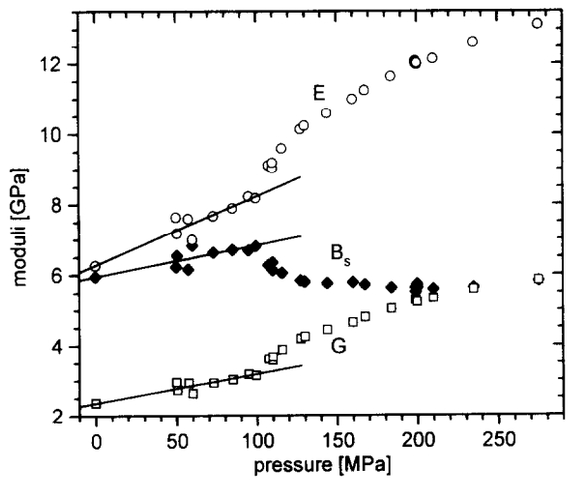

Figure 5 Shear modulus G (□), Young's modulus E (○) and bulk modulus B_s (◆) *versus* pressure. The lines represent linear fits (slopes given in *Table 3*)

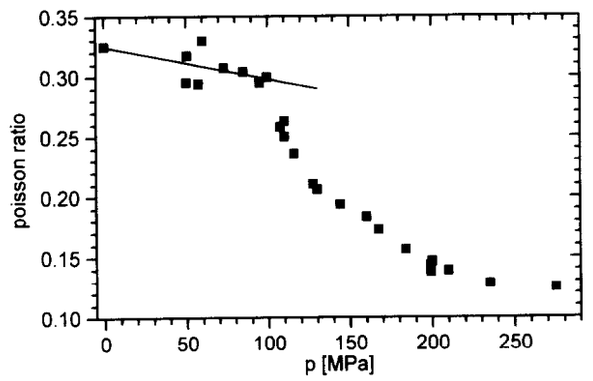

Figure 6 Poisson's ratio *versus* pressure. The solid line represents a linear fit (slope given in *Table 3*)

Table 3 Slopes of the pressure dependence of properties at zero applied pressure

$dB_s/dp\|_{p=0}$	8.85
$dc_{11}/dp\|_{p=0}$	18.8
$dc_{44}/dp\|_{p=0}$	8.19
$dE/dp\|_{p=0}$	19.5
$d\nu/dp\|_{p=0}$ (GPa^{-1})	−0.265

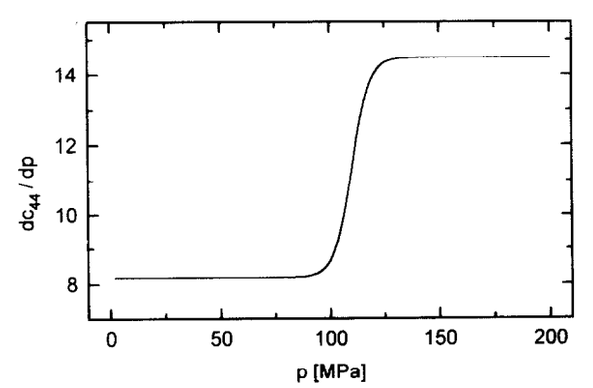

Figure 7 Fit of the slope of c_{44} *versus* pressure, equation (13)

dilation is now necessary for any uniaxial deformation. The slopes of the moduli and Poisson's ratio *versus* pressure curves at ambient pressure are given in *Table 3*.

DISCUSSION

Ignoring the intensity changes of the transverse phonons, all peculiarities observed are due to the change of slope of c_{44} *versus* pressure. A fit of the slope of c_{44} *versus* pressure

$$\frac{\partial c_{44}}{\partial p} = (s_1 - s_2)\left(1 + \exp\frac{p - p_0}{\Delta p}\right)^{-1} + s_2 \qquad (13)$$

is displayed in *Figure 7*. It exhibits the classical step of a second-order phase or a glass transition. The constants are given in *Table 4*.

It is important to note that c_{11} shows no trace of such a behaviour. The plot of c_{11} *versus* density shown in *Figure 8* is strictly linear over the whole range covered. The slope of 0.0778 (10^9 N m kg^{-1}) in the density range from 1190 to 1290 kg m^{-3} obtained by pressure changes well compares with 0.0758 (10^9 N m kg^{-1}) obtained within a 2 kg m^{-3} range by changing the temperature[12].

Looking at the shear modulus and the Pockels coefficient, the intuitive interpretation is that *increasing the pressure leads to increased correlation between shear movements and local rotation* motions due to the closer packing. It seems that at 110 MPa a sudden increase of cooperativity creates a new situation. The downstep of the bulk modulus also points to a cooperative phenomenon facilitating compression. The Poisson's ratio, on the other hand, shows that this cooperativity is an obstacle for uniaxial deformation. Beyond this pressure a unique behaviour exists that can be extrapolated down to zero pressure. Any interpretation of this detail must remain pure speculation at the present time.

The question arises whether our findings and intuitive interpretation fit the general picture accepted for the glass transition and the glassy state. Several explanations seem to be at hand.

Table 4 Numerical values of parameters in equations (11) and (13)

p_0 (MPa)	110
Δp (MPa)	4
s_1	8.1
s_2	14.5

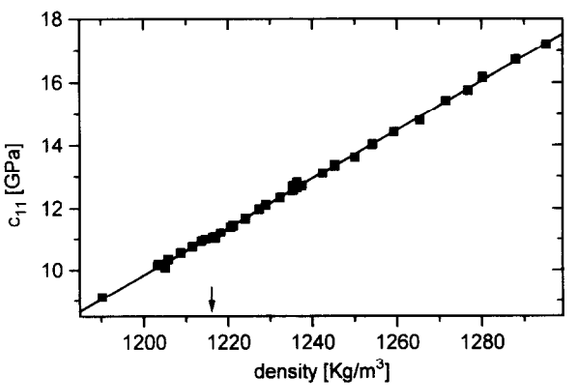

Figure 8 Plot of c_{11} *versus* density. The line represents a linear fit (slope = 0.0778 × 10^{-9} N m kg^{-1}). The density corresponding to the step in c_{44} is indicated by the arrow

(1) A secondary relaxation taking place below the glass transition temperature (T_g) could be invoked to explain the observations. However, the known processes[13] have frequencies that are too low at room temperature. Pressure is known to shift the whole activation diagram to higher temperatures[14] as indicated schematically in *Figure 9*. Thus lower frequencies enter the temperature window. Only the δ-relaxation attributed to the side-chain CH_3 groups cannot immediately be ruled out. However, even down to liquid helium temperatures no observation of shear waves in PMMA has been reported[15], meaning that the frequency–temperature superposition principle—if applicable at all—gives no hint. If our findings can be corroborated with other polymeric glasses an *ad hoc* molecular interpretation could be excluded.

(2) The β-process of mode coupling theory in its simple form can be ruled out since it is situated on the liquid side of T_g. Moreover, only density-mode coupling is considered. Thus it provides no explanation for the shear effect on the solid side of T_g.

(3) Generalized mode coupling, such as a combination of density-mode coupling and spin-mode coupling, leads to an additional glass transition within the glassy state[16]. It appears to be a natural extension of the mode coupling concept to consider shear-mode coupling in dense phases, where shear waves exist. The density-mode coupling leads to the primary glass transition manifested *inter alia* as a step of the bulk modulus. Consequently shear-mode coupling should lead to a step in the shear modulus such as that observed here. If these observations can be repeated, then this must be a quite general phenomenon in solids, depending only on the appearance of mode coupling. It can be speculated that this is a property of disordered solids in contrast to crystals.

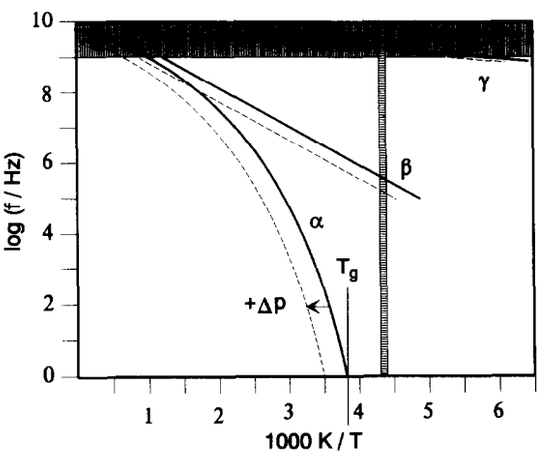

Figure 9 Principal relaxation map showing the shift of different relaxation processes with pressure. The arrow shows the shift from ambient (bold lines) to higher pressure (dashed lines). The vertical hatched area is the frequency range accessible by Brillouin scattering, the horizontal hatched area is the temperature range of the experiment. Only phenomena in this region can be observed by Brillouin scattering

(4) A real phase transition: ordering of tactic sequences of the PMMA chain may occur, resulting in some kind of condis-crystal. This should lead to other observable effects. It appears that such behaviour should generally be restricted to glasses of linear chain molecules.

The considerations presented above clearly indicate that more work should be done in this field.

ACKNOWLEDGEMENT

The authors thank the Deutschen Forschungsgemeinschaft for partial financial support within the Sonderforschungsbereich 239 Projekt B9.

REFERENCES

1 Goldbach, G. and Rehage, G. *Rheol. Acta* 1967, **6**, 30
2 Ngoepe, P. E., Lambson, E. F., Saunders, G. A. and Bridge, B. *J. Mater. Sci.* 1990, **25**, 4654
3 Dollhopf, W., Barry, S. and Strauss, M. J. in 'Frontiers of High-Pressure Research' (Eds H. D. Hochheimer, R. D. Etters), Plenum Press, New York, 1991
4 Atkins, P. W. 'Physical Chemistry', Oxford University Press, Oxford, 1978
5 Hochheimer, H. D., Shand, M. L., Potts, J. E., Hanson, R. C. and Walker, C. T. *Phys. Rev. B* 1976, **14**, 4630
6 Krüger, J. K., Peetz, L. and Pietralla, M. *Polymer* 1978, **19**, 1397
7 Krbecek, H., Krüger, J. K. and Pietralla, M. *J. Polym. Sci. B, Polym. Phys. Edn* 1993, **31**, 1477
8 Peercy, P. S., Samara, G. A. and Morosin, B. *J. Phys. Chem. Solids* 1975, **36**, 1123
9 Mazzacurati, V., Nardone, M., Ruocco, G. and Signorelle, G. in 'Dynamics of Disordered Materials' (Eds D. Richter, A. J. Dianoux, W. Petry and J. Teixeira), Springer, Berlin, 1988
10 Peetz, L., Krüger, J. K. and Pietralla, M. *Colloid Polym. Sci.* 1987, **256**, 761
11 Durvasula, L. N. and Gammon, R. W. *J. Appl. Phys.* 1979, **50**, 4339
12 Roberts, R. *Thesis*, Universität Saarbrücken, 1985
13 McCrum, N. G., Read, B. E. and Williams, G. 'Anelastic and Dielectric Effects in Polymeric Solids', John Wiley & Sons, London, 1967
14 Koppelmann, J. *Österr. Kunstoff-Zeitschrift* 1972, **9/10**, 173
15 Schmidt, M., Vacher, R., Pelous, J. and Huncklinger, S. *J. de Physique* 1982, **43**, C9–501
16 Götze, W. and Haussmann, R. *Z. Phys. B—Condensed Matter* 1988, **72**, 403